climate

MDPI

Article

Climate Change and Thermal Comfort in Greece

Harry D. Kambezidis [1,*], Basil E. Psiloglou [2], Konstantinos V. Varotsos [2] and Christos Giannakopoulos [2]

[1] Atmospheric Research Team, Institute of Environmental Research and Sustainable Development, National Observatory of Athens, GR-11810 Athens, Greece
[2] Institute of Environmental Research and Sustainable Development, National Observatory of Athens, GR-15236 P. Penteli, Greece; bill@noa.gr (B.E.P.); varotsos@noa.gr (K.V.V.); cgiannak@noa.gr (C.G.)
* Correspondence: harry@noa.gr

Abstract: Global warming is an environmental issue keeping all nations alert. Under this consideration, the present work investigates the future thermal sensation of the Greek population. Three periods are selected (2021–2050, 2046–2075, 2071–2100) and two Intergovernmental Panel for Climate Change (IPCC) representative concentration pathway (RCP) 4.5 and 8.5 scenarios. Use of Thom's discomfort index (TDI) is made, which is calculated from air temperature and relative humidity included in typical meteorological years (TMYs) derived for 1985–2014 and future periods (both IPCC scenarios) for 33 locations in Greece. TDI is discriminated into 6 classes. The analysis shows that there is no significant shift from past to future annual mean TDIs in terms of its classification. The same is found for the summer TDI values. Nevertheless, a distribution of the various TDI classes is provided within the TMYs. Maps of annual TDI values are prepared for Greece by using the kriging method; higher values are found in the southern part of Greece and lower values in the northern. Best-fit regression equations derived show the intra-annual TDI variation in all periods. Also, scatter plots of annual TDIs in the future epochs in comparison with the historical period show a linear relationship.

Keywords: climate change; global warming; thermal comfort; Thom's Discomfort Index; Greece

Citation: Kambezidis, H.D.; Psiloglou, B.E.; Varotsos, K.V.; Giannakopoulos, C. Climate Change and Thermal Comfort in Greece. *Climate* **2021**, *9*, 10. https://doi.org/10.3390/cli9010010

Received: 16 December 2020
Accepted: 4 January 2021
Published: 8 January 2021

1. Introduction

The global-warming phenomenon is impacting the surface temperature of the Earth. Indeed, the Intergovernmental Panel for Climate Change (IPCC) [1] highlights that each of the recent 3 decades has become warmer than any other period prior to 1980. Also, the National Oceanic and Atmospheric Administration (NOAA) [2] reports that the 10 warmest years on record at global scale have appeared after 1998. Therefore, it is common sense that the increase in temperature may result in more frequent heat stresses (thermal discomfort) upon people [3–6], thus affecting the quality of life. This issue has, therefore, been the subject of several studies; these studies are focused on either the thermal comfort of people indoors (within a building) or outdoors (ambient conditions). For expressing the thermal comfort (or alternatively the thermal discomfort), several indices have been developed.

Yang et al. [7] have studied the thermal comfort during winter at the city of Tianjin, N. China. Adegoke and Dombo [8] examined the human thermal comfort in Akure, Nigeria. Cohen et al. [9] investigated the thermal perception in the urban web of Tel Aviv, Israel. Epstein and Moran [10] compared indices for thermal comfort and heat stress (extreme thermal discomfort). Golasi et al. [11] compared the Mediterranean outdoor comfort index (MOCI), as well as the predicted mean vote (PMV), and the popular events tracking (PET) models in Rome and found that the most appropriate is MOCI. A similar study was performed at Chiba, Japan, by comparing the models of PET, PMV, and standard effective temperature (SET) [12]. The outdoor thermal comfort was also studied in a subarctic climate of north Sweden [13]. Yousif and Tahir [14] investigated the thermal effect on people in Khartoum, Sudan. An informative review about the thermal effect on people has been given by Djongyang et al. [15].

Specifically, for Greece there have been several studies about the effect of heat on the population. Angouridakis and Makrogiannis [16] found the environmental thermal sensation for summer in Thessaloniki by analysing air-temperature and relative-humidity data in the period 1950–1957. Giles et al. [17] studied the heat stress in Athens and Thessaloniki during the heat waves of 1987 and 1988. Paliatsos and Nastos [18] compared the thermal effect during air-pollution episodes in Athens for the summers of 1993–1995 and found that it was related to the ozone concentration. Tselepidaki et al. [19] examined the summer thermal perception in Athens for cooling purposes. Tsitoura et al. [20] performed outdoors questionnaire about the thermal-comfort effect on people in 4 cities of Crete. Stathopoulou et al. [21] calculated the thermal effect from satellite-derived meteorological data and compared it with that from in situ measurements. Pantavou et al. [22] used various thermal-comfort indices in Athens (see their Table 2). Also, Pantavou [23] estimated the thermal sensation of pedestrians in 4 locations of Athens. Katavoutas and Founda [24] examined the period of 1960–2017 and found an increasing risk of heat stress in Athens.

It is obvious from the above works that no study about the thermal comfort has been conducted worldwide for a whole region or country. Therefore, the present work aims at filling this gap in the case of Greece. A second innovation of the study is the use of typical meteorological years (TMYs); such TMYs have been developed for 33 sites in Greece [25].

The work is divided into Sections. Section 2 deploys the data collection and analysis. Section 3 gives the results of the study. Section 4 provides a discussion and Section 5 deploys the main conclusions of the study.

2. Materials and Methods

According to [25] "A TMY is a set of meteorological and irradiance parameters usually consisting of hourly values in a year for a given geographical location (https://e3p.jrc.ec.europa.eu/articles/typical-meteorological-year-tmy). Furthermore, a TMY consists of a set of typical meteorological months (TMMs) selected from individual years integrated into a complete year. A TMY reflects all the climatic information of the location for a period as long as the mean life of the system." The aim of that study [25] was the development of TMYs for 5 different applications, i.e., TMY-meteorology-climatology (TMY-MC), TMY-bio-meteorology (TMY-BM), TMY-agro-meteorology-hydrology (TMY-AMH), TMY-PV applications (TMY-PV), and TMY-energy design of buildings (TMY-EDB); all these TMYs were generated for 33 sites in Greece in the frame of the "Development of synergistic and integrated methods and tools for monitoring, management and forecasting of environmental parameters and pressures" (KRIPIS-THESPIA-II) funded project, by using historical data of various meteorological parameters in the period 1985–2014 (30 years). During this project, TMYs-MC were also derived for future periods (2021–2050, 2046–2075, 2071–2100) for all 33 locations, not yet published. The future TMYs-MC considered two opposing IPCC scenarios, i.e., the representative concentration pathway (RCP) 4.5 (intermediate scenario with an "anthropogenic" radiative forcing of 4.5 Wm^{-2} in the year 2100) and the RCP 8.5 (extreme scenario with an "anthropogenic" radiative forcing of 8.5 Wm^{-2} in the year 2100). For the TMY-generation statistical procedure one may refer to [25]. Since TMYs-MC have been derived for both the historical and the future time periods, they are used in the present work.

The historical TMYs-MC consist of hourly mean values of dry-bulb temperature (in °C), relative humidity (in %), atmospheric pressure (in hPa), and global horizontal irradiance (in Wm^{-2}) at the sites' altitude, while the future TMYs contain daily mean values of these parameters. To display the thermal comforts (or discomforts) across Greece for the historical and future periods and compare them, use of Thom's discomfort index (TDI in °C) has been made [26]. Its definition is as follows.

$$TDI = T_d - 0.55\,(1 - 0.01\,RH)\,(T_d - 14.5), \quad (1)$$

where T_d is the dry-bulb temperature (in °C) and RH the relative humidity (in %). Thom defined a series of limits for TDI; these are given in Table 1.

Table 1. Description, classes and ranges of Thom's discomfort index (TDI) [26].

Description	TDI Class	Range (°C)
No discomfort	A	<21
Under 50% of the population feels discomfort	B	21–23.99
Over 50% of the population feels discomfort	C	24–26.99
Most of the population feels discomfort	D	27–28.99
Everyone feels discomfort	E	29–31.99
State of medical emergency	F	≥32

Therefore, hourly values of TDI were calculated from the corresponding values of T_d and RH in the historical TMYs-MC and daily values in the future TMYs-MC for the 33 sites in Greece. These locations cover all of Greece and are given in Table 2; a map with the location of the 33 sites is also shown in Figure 1. The meteorological data for the 33 sites in the historical period 1985–2014 have been obtained from the Hellenic National Meteorological Service (HNMS) network, while the corresponding global horizontal irradiance values have been derived through the meteorological radiation model (MRM) code [27,28]. From these 33 data bases the historical TMYs-MC have been generated. As far as the future TMYs-MC are concerned, data for the closest grid point to the HNMS station's location were employed from a transient realisation of the regional climate model RCA4 of the Swedish Meteorological and Hydrological Institute (SMHI) ([29], and references therein) driven by the Earth system model of the Max Planck Institute for Meteorology (MPI-M) [30]; simulations were carried out in the framework of the European Coordinated Regional Climate Downscaling Experiment (EURO-CORDEX) modelling experiment (http://www.euro-cordex.net). The horizontal resolution of the RCA4 model was 0.11° (~12 × 12 km). The meteorological and global horizontal radiation data for the future periods 2021–2050, 2046–2075, and 2071–2100 were provided from ECO-CORDEX to the KRIPIS-THESPIA-II project; therefore, corresponding TMYs-MC were derived following the statistical procedure described in [25]. The presentation of these future TMYs-MC will be the subject of a separate publication, which is in preparation.

Table 2. Meteorological sites of the Hellenic National Meteorological Service (HNMS) network used in this study.

Nr.	Station Name [1] (Region in Greek/English language) [1]	Station's World Meteorological Organisation code (16xxx)	Latitude (deg N)	Longitude (deg E)	Elevation (m amsl)
1	Serres (Kentriki Makedonia/Central Macedonia)	606	41.083	23.567	34.5
2	Kastoria (Dytiki Makedonia/Western Macedonia)	614	40.450	21.283	660.9
3	Mikra, outskirts of Thessaloniki (Kentriki Makedonia/Central Macedonia)	622	40.517	22.967	4.8
4	Alexandroupoli (Anatoliki Makedonia and Thraki/Eastern Macedonia and Thrace)	627	40.850	25.933	3.5
5	Kozani (Dytiki Makedonia/Western Macedonia)	632	40.283	21.783	625.0
6	Kerkyra, known as Corfu (Ionioi Nisoi/Ionian Islands)	641	39.617	19.917	4.0
7	Ioannina (Ipiros/Epirus)	642	39.700	20.817	484.0
8	Larisa (Thessalia/Thessaly)	648	39.650	22.450	73.6
9	Limnos (Voreio Aigaio/Northern Aegean)	650	39.917	25.233	4.6
10	Anchialos (Thessalia/Thessaly)	665	39.217	22.800	15.3
11	Lesvos (Voreio Aigaio/Northern Aegean)	667	39.067	26.600	4.8
12	Agrinio (Dytiki Ellada/Western Greece)	672	38.617	21.383	25.0
13	Lamia (Sterea Ellada)	675	38.850	22.400	17.4
14	Andravida (Dytiki Ellada/Western Greece)	682	37.917	21.283	15.1
15	Skyros (Sterea Ellada)	684	38.900	24.550	17.9
16	Araxos (Dytiki Ellada/Western Greece)	687	38.133	21.417	11.7
17	Tanagra (Sterea Ellada)	699	38.317	23.550	139.0
18	Chios (Voreio Aigaio/Northern Aegean)	706	38.350	26.150	4.0
19	Tripoli (Peloponissos/Peloponnese)	710	37.533	22.400	652.0

Table 2. *Cont.*

Nr.	Station Name [1] (Region in Greek/English language) [1]	Station's World Meteorological Organisation code (16xxx)	Latitude (deg N)	Longitude (deg E)	Elevation (m amsl)
20	Elliniko (Attica)	716	37.900	23.750	15.0
21	Zakynthos, known as Zante (Ionioi Nisoi/Ionian Islands)	719	37.783	20.900	7.9
22	Samos (Voreio Aigaio/Northern Aegean)	723	37.700	26.917	7.3
23	Kalamata (Peloponissos/Peloponnese)	726	37.067	22.000	11.1
24	Naxos (Notio Aigaio/Southern Aegean)	732	37.100	25.533	9.8
25	Methoni (Peloponissos/Peloponnese)	734	36.833	21.700	52.4
26	Spata (Attiki/Attica)	741	37.967	23.917	67.0
27	Kythira (Attiki/Attica)	743	36.133	23.017	166.8
28	Thira, known as Santorini (Notio Aigaio/Southern Aegean)	744	36.417	25.433	36.5
29	Souda (Kriti/Crete)	746	35.550	24.117	140.0
30	Rodos, known as Rhodes (Notio Aigaio/Southern Aegean)	749	36.400	28.117	11.5
31	Irakleio, also written as Heraklion (Kriti/Crete)	754	35.333	25.183	39.3
32	Siteia (Kriti/Crete)	757	35.120	26.100	115.6
33	Kasteli (Kriti/Crete)	760	35.120	25.333	335.0

[1] The names have been converted into Latin characters from the Greek alphabet according to the Hellenic Standardisation Organisation (ELOT) 743 standard [31], which is the adoption of the ISO 843 one [32].

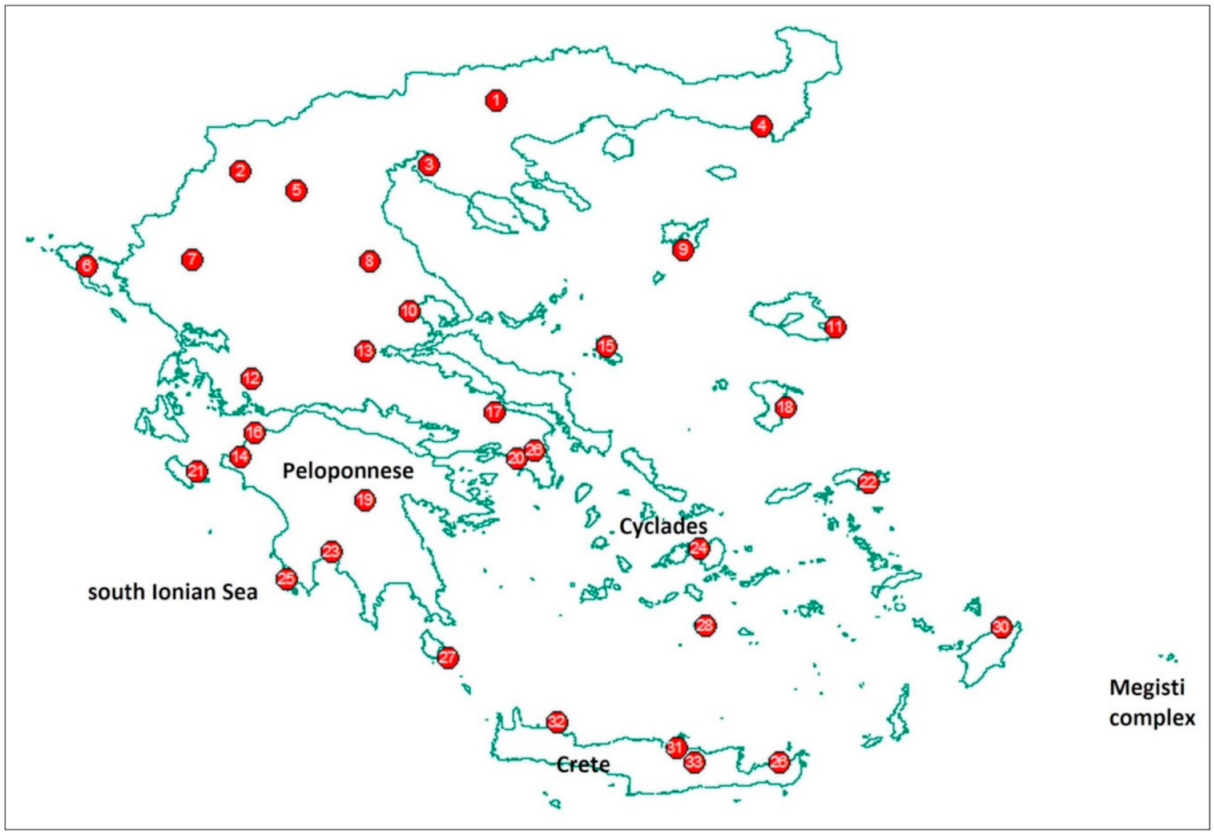

Figure 1. Distribution of the 33 selected HNMS stations (red circles) over Greece. The numbers within the circles refer to their names in column 1 of Table 2. The regions of south Ionian Sea, Peloponnese, the Cyclades (islands), Crete, and Megisti complex (of islands) are also shown; the Megisti complex is also known as the Kastellorizo complex, a complex of 14 small islands/rocky islets.

3. Results

This section is divided in sub-Sections according to the time scale encountered (annual, seasonal, monthly). As far as the seasonal analysis is concerned, this is performed for the summer time (June, July, August—JJA), as it is the one which may affect people negatively because of high ambient temperatures [19] or even heatwaves [17,33]. As mentioned in Section 2, two IPCC scenarios have been adopted in this work. The first is the IPCC RCP 4.5 (stabilisation) scenario; according to it a global temperature increase by 2100 is in the order of 1.7–3.2 °C. The second is the IPCC RCP 8.5 (high-end) scenario, which foresees a global temperature increase in the range of 3.2–5.4 °C.

As mentioned in Sections 1 and 2, use of the derived TMYs for the 33 sites in Greece (both historical and future) has been made in this study. Under this situation, analysis of the TDI tendency during the historical and future periods cannot be done because these long periods have been substituted by a single year (a TMY). As a TMY is a representative year climate-wise for the period from which it has come, so are the TDIs derived this way. Another reason for this controversy is the fact that the TMMs that comprise a single TMY come from different years of the period considered (see Table 3 as example where 4 sites have arbitrarily been chosen). On the other hand, comparison between the historical and future TDIs cannot directly be made because the historical TDIs are hourly values, while the future ones are daily values.

Table 3. The HNMS stations of Agrinio, Irakleio, Kastoria, and Tripoli with their typical meteorological months (TMMs) selected from years within the period 1985–2014.

Station	Jan	Feb	Mar	Apr	May	Jun	Jul	Aug	Sep	Oct	Nov	Dec
Agrinio	1999	2004	2000	1994	2001	1997	2000	1999	2004	1988	2010	1994
Irakleio	1995	2001	2004	1994	1997	1987	2003	1996	1996	1997	2004	2003
Kastoria	1987	1988	2005	1985	1995	1996	1996	1998	1991	1994	1989	2008
Tripoli	1999	1985	1993	1993	1995	1987	1987	1986	1986	1991	2004	1994

3.1. Annual Thom's Discomfort Index (TDI) Values

Figure 2 shows the annual mean TDI values for all 33 sites in Greece. It is seen, as anticipated, that the RCP 8.5 scenario produces greater spread of the annual values among the various epochs in comparison with the RCP 4.5 scenario. To show this effect in a better way, differences between the future annual mean TDI values and those in the historical period have been calculated. Figure 3 provides the annual mean differences ΔTDIs = $TDI_{\text{future epoch}} - TDI_{\text{historical period}}$. Under the RCP 4.5 scenario the increase in the absolute TDI values is of the order of 0.1–1.7 °C approximately, considering all 3 future epochs. It is interesting to see that the sites of Elliniko and Ioannina present negative differences in all 3 periods, while Kasteli and Lamia in the first future period only, and Naxos and Thira in the first 2 future epochs; this means that their population will experience a "milder" thermal sensation in the future. By contrast, the RCP 8.5 scenario demonstrates an apparent increase in the thermal sensation across Greece in the range of almost 0.4–3.5 °C. Some stations (Elliniko, Ioannina, Kasteli, Kerkyra, Lamia, Naxos, Thira), however, present a dissonance as far as the first (2021–2050) future epoch is concerned, as done in the RCP 4.5 scenario also. Anyhow, in both scenarios, the average annual increase in TDI implies even higher TDI values on the daily or even hourly scale, which can be related to persistent and more intense heat waves that may occur in the future. Table 4 shows the difference between the annual mean TDI values for all sites and periods considered.

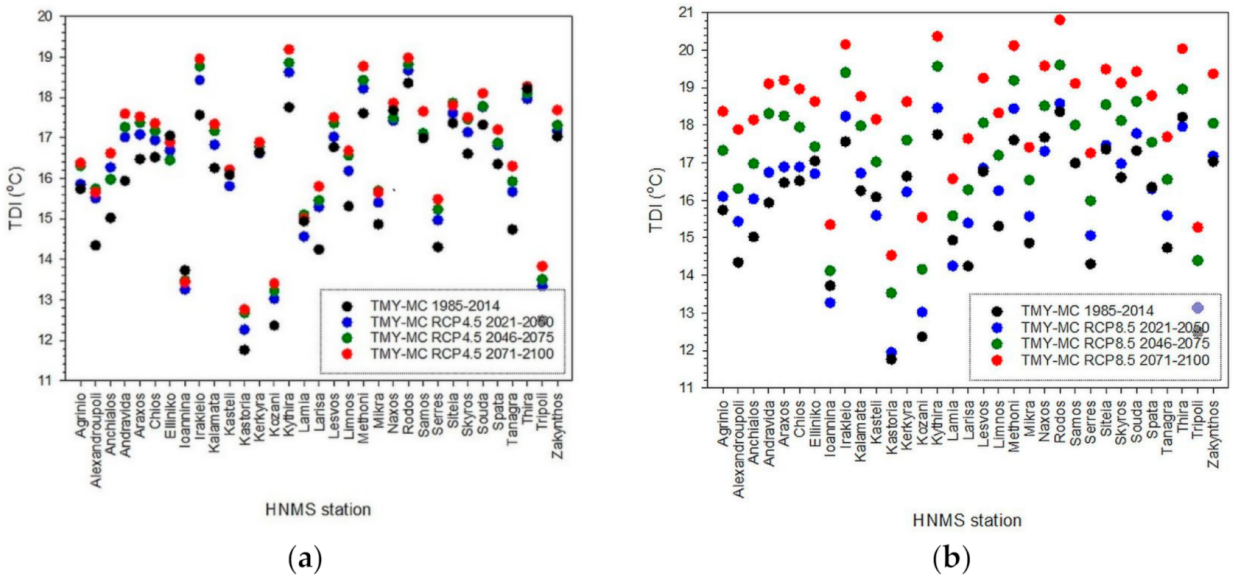

Figure 2. Annual mean TDI values for all HNMS sites (in alphabetical order) as derived from the typical meteorological years -meteorology-climatology (TMYs-MC) during the historical period of 1985–2014 and the future epochs of 2021–2050, 2046–2075, 2071–2100 under the (**a**) representative concentration pathway (RCP) 4.5 and (**b**) RCP 8.5 Intergovernmental Panel for Climate Change (IPCC) scenarios.

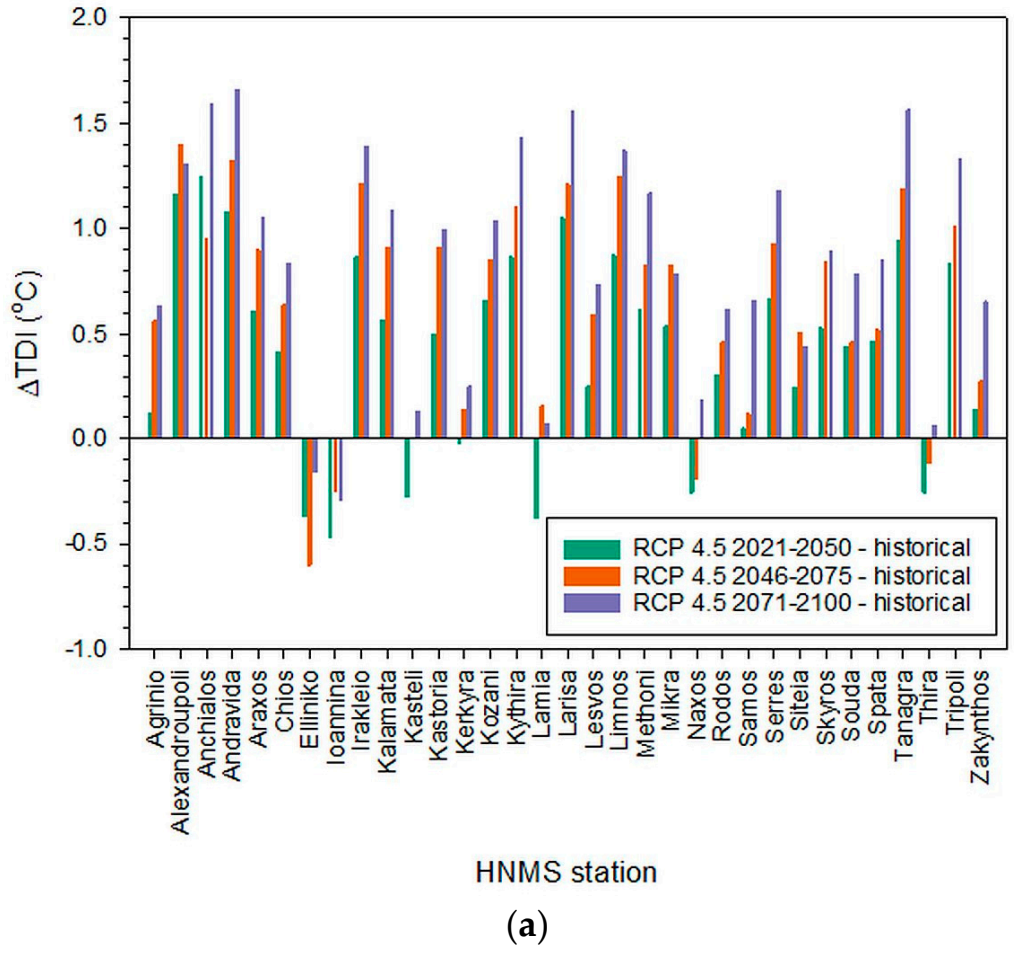

Figure 3. *Cont.*

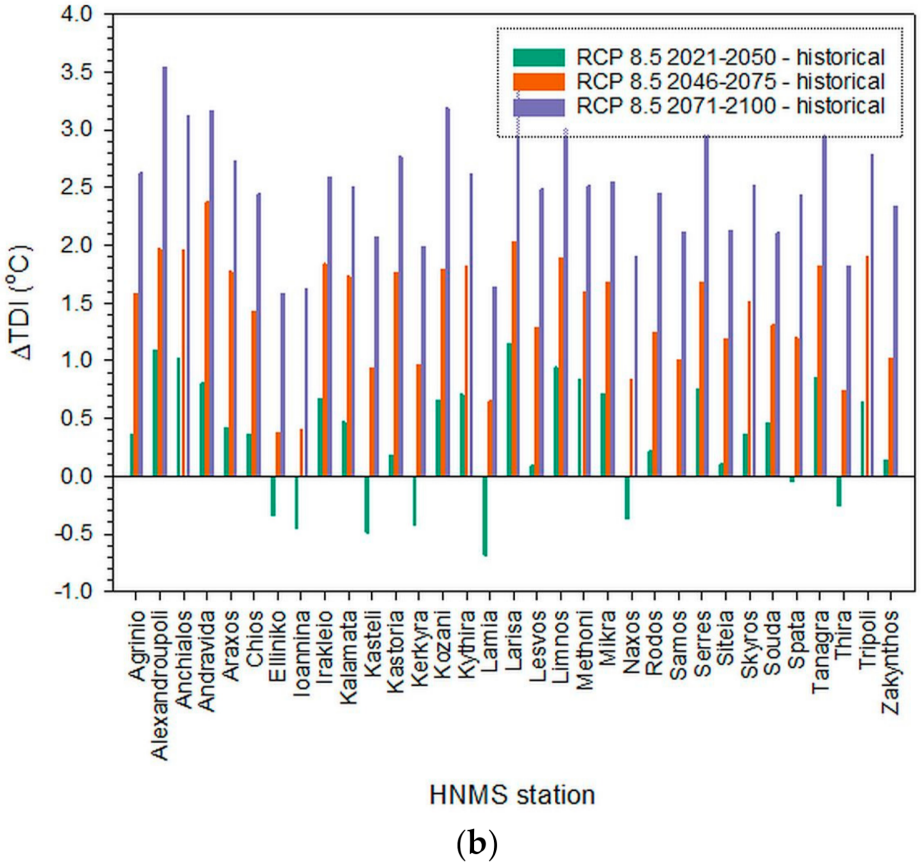

(**b**)

Figure 3. Annual mean ΔTDIs for all HNMS sites (in alphabetical order) as derived from the TMYs-MC during the historical period of 1985–2014 and the future epochs of 2021–2050, 2046–2075, 2071–2100 under the (**a**) RCP 4.5 and (**b**) RCP 8.5 IPCC scenarios. The definition of ΔTDI is given in the text.

Table 4. Average annual TDI (in °C) and average annual ΔTDI (in °C) values for all sites and periods considered; the standard deviation from the mean is shown in parenthesis. The definition of ΔTDI is given in the text.

Parameter	Period						
	Historical 1985–2014	**RCP 4.5 2021–2050**	**RCP 4.5 2046–2075**	**RCP 4.5 2071–2100**	**RCP 8.5 2021–2050**	**RCP 8.5 2046–2075**	**RCP 8.5 2071–2100**
Annual average TDI	15.89 (±1.70)	16.32 (±1.63)	16.52 (±1.60)	16.74 (±1.65)	16.22 (±1.64)	17.33 (±1.60)	18.40 (±1.54)
Annual average ΔTDI	0	0.43 (±0.48)	0.64 (±0.51)	0.85 (±0.54)	0.33 (±0.51)	1.44 (±0.50)	2.51 (±0.51)

If one considers the centres of each 30-year period in Table 4, being the years 2000, 2035, 2060, and 2085, respectively, then the corresponding increase in TDI is found to be ≈0.12 °C/decade, ≈0.11 °C/decade, ≈0.10 °C/decade for the 3 periods under the IPCC RCP 4.5 scenario, and ≈0.09 °C/decade, ≈0.24 °C/decade, ≈0.30 °C/decade for the respective periods under the IPCC RCP 8.5 scenario. Such increases are considered insignificant in terms of the thermal sensation of the Greek population because they do not shift the thermal (dis)comfort from class A to a higher one, since all average annual TDIs lie in the TDI-class A (see Table 1).

3.2. Summer TDI Variation

In a similar way to what was presented in Figure 3, Figure 4 shows the summer differences between the future TDI values and the historical ones ($\Delta TDI = TDI_{\text{future epoch}} - TDI_{\text{historical period}}$). From these figures the following observations can be made: (i) many sites seem to have a better summer thermal sensation (negative ΔTDIs) mostly in the RCP 4.5 2046–2075 period and less in the RCP 4.5 2021–2050 one (Figure 4a); (ii) higher annual

absolute ΔTDIs values of almost 0.5 °C are found under both IPCC scenarios than their respective annual TDI ones (cf. Figure 3); this implies an abrupt increase in the future thermal (dis)comfort at these sites.

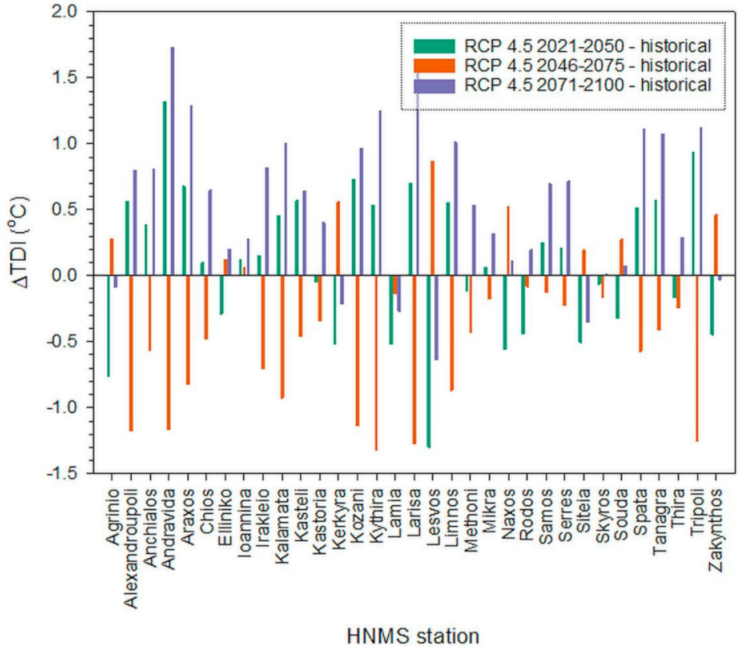

(**a**)

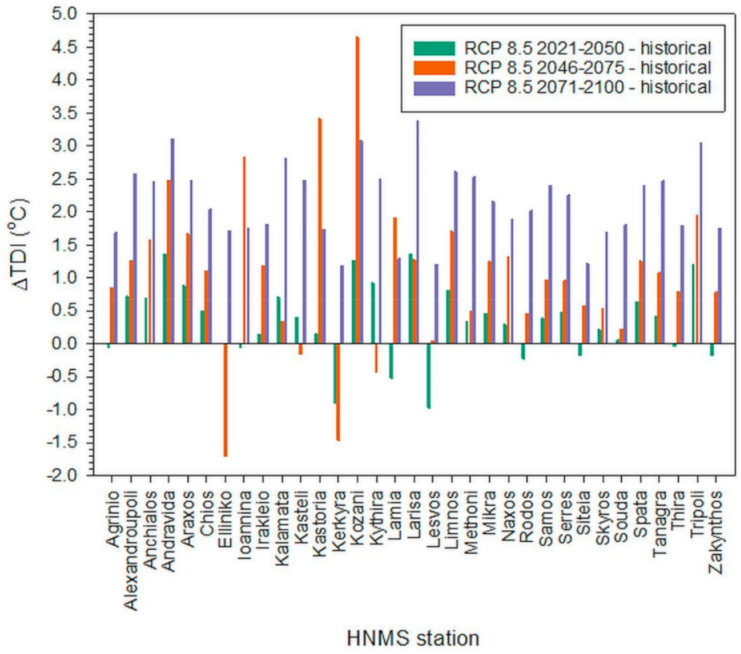

(**b**)

Figure 4. Summer (JJA) mean ΔTDIs for all HNMS sites (in alphabetical order) as derived from the TMYs-MC during the historical period of 1985–2014 and the future epochs of 2021–2050, 2046–2075, 2071–2100 under the (**a**) RCP 4.5 and (**b**) RCP 8.5 IPCC scenarios. The definition of ΔTDI is given in the text.

By repeating the values of Table 4 for the summer case, Table 5 is derived.

Table 5. Average summer TDI (in °C) and average summer ΔTDI (in °C) values for all sites and periods considered; the standard deviation from the mean is shown in parenthesis. The definition of ΔTDI is given in the text.

Parameter	Period						
	Historical 1985–2014	**RCP 4.5 2021–2050**	**RCP 4.5 2046–2075**	**RCP 4.5 2071–2100**	**RCP 8.5 2021–2050**	**RCP 8.5 2046–2075**	**RCP 8.5 2071–2100**
Summer average TDI	22.37 (±1.02)	22.47 (±0.81)	22.72 (±0.83)	22.91 (±0.91)	22.71 (±0.86)	23.43 (±0.87)	24.53 (±0.88)
Summer average ΔTDI	0	0.10 (±0.56)	0.35 (±0.59)	0.55 (±0.58)	0.34 (±0.58)	1.07 (±1.22)	2.16 (±0.58)

It is understandable that the summer thermal feeling throughout Greece both in the present and the future is in class B as all mean TDI values vary in the range 21–23.99; the exception is the RCP 8.5 2071–2011 period, which shifts to TDI-class C (24–26.99 °C). Calculations of the trends of TDI during summertime as done for its annual values result in the following conclusions: an increase in TDI of ≈0.03 °C/decade, ≈0.06 °C/decade, ≈0.06 °C/decade for the 3 periods under the IPCC RCP 4.5 scenario, and ≈0.10 °C/decade, ≈0.18 °C/decade, ≈0.25 °C/decade for the respective periods under the IPCC RCP 8.5 scenario. Such increases are considered insignificant in terms of the thermal sensation of the Greek population during summertime because they do not shift the thermal (dis)comfort from class B to a higher one, except for the RCP 8.5 2071–2100 period, which is classified in TDI-class C. Nevertheless, many sites seem to experience milder thermal feeling in the future than now as their ΔTDIs are negative in both RCP scenarios as shown in Figure 4a,b. Another interesting observation from Table 5 is that the average summer TDI values of RCP 4.5 2021–2050 (22.47 °C) and RCP 8.5 2046–2075 (22.43 °C) are almost equal; the same happens to the *TDI* values of the periods RCP 4.5 2046–2075 (22.72 °C) and RCP 8.5 2021–2050 (22.71 °C).

3.3. Intra-Annual TDI Variation

There is always a question about the in-year variability of a meteorological quantity. The quantity in question in this study is TDI, although it is not an immediate meteorological parameter but a derivative from ambient temperature and relative humidity. Figure 5 shows this variation for all periods of the study. A best-fit curve has also been derived for each case and can be used to calculate the average monthly TDI in Greece. The monthly TDI values in Figure 5 are averages over the 33 sites.

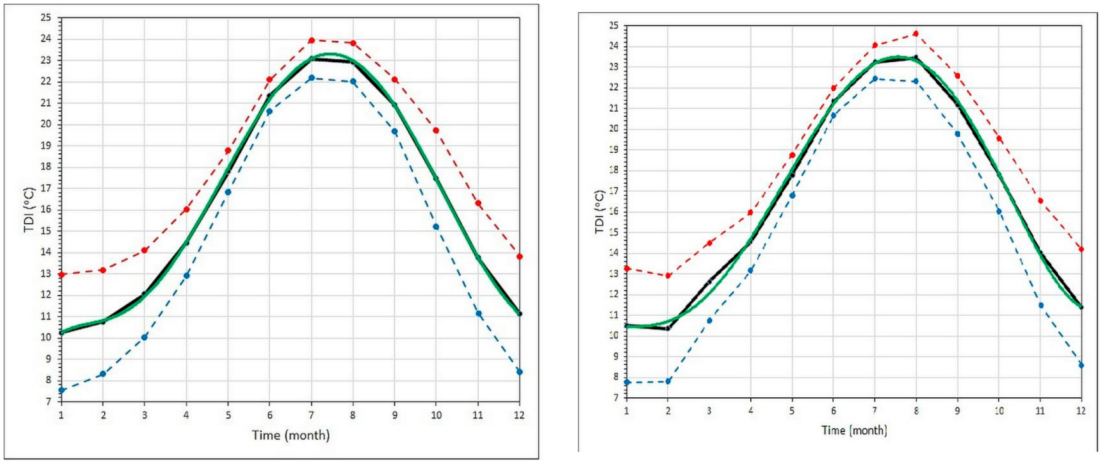

(**a**) (**b**)

Figure 5. *Cont.*

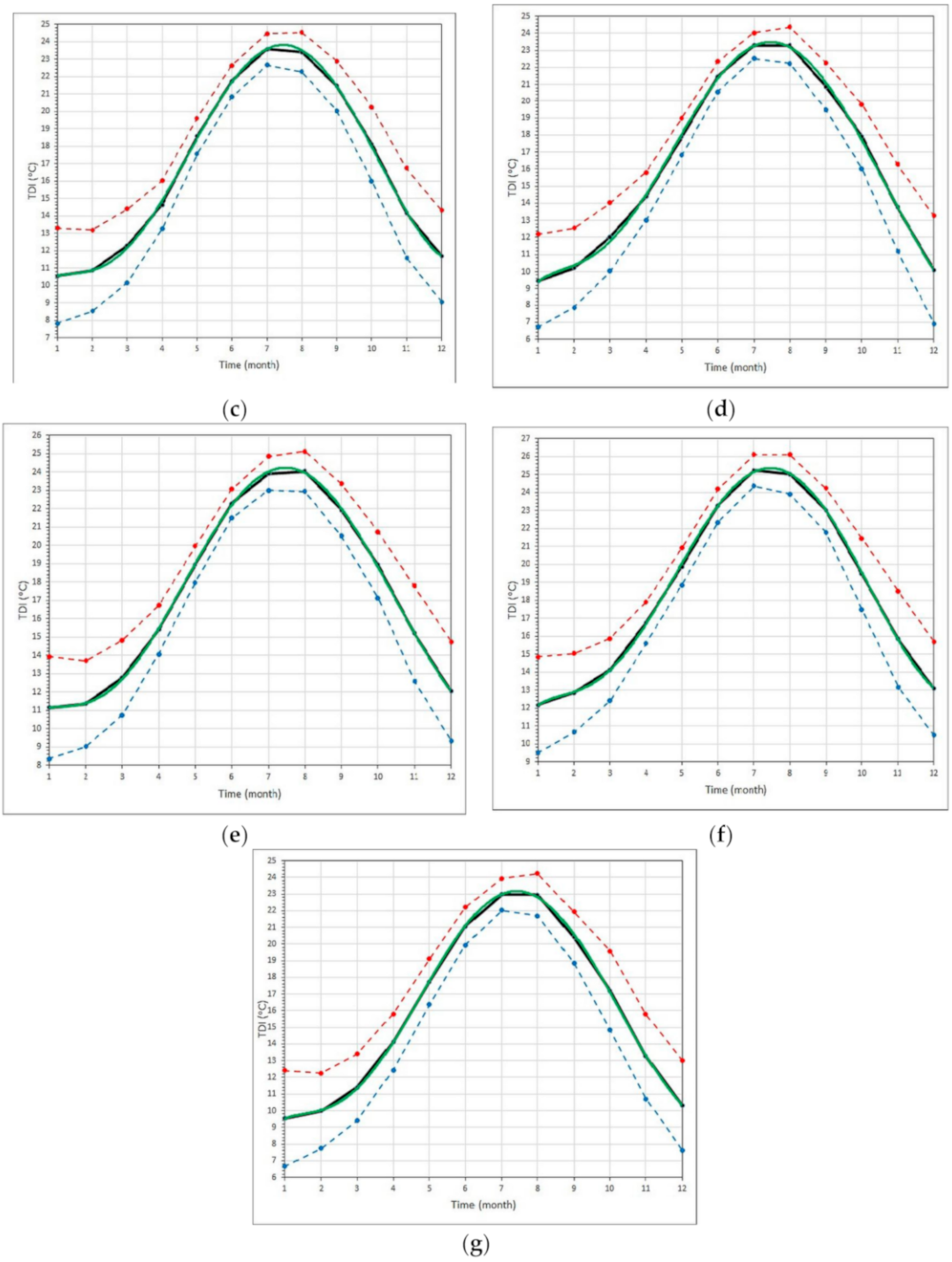

Figure 5. Intra-annual variation of the monthly mean TDIs in the epochs: (**a**) RCP 4.5 2021-2050, (**b**) RCP 4.5 2046–2075, (**c**) RCP 4.5 2071–2100, (**d**) RCP 8.5 2021–2050, (**e**) RCP 8.5 2046–2075, (**f**) RCP 8.5 2071–2100, and (**g**) historical 1985–2014. The black solid lines are the monthly means, the green solid curves are the best-fit polynomial lines to the means, and the red and blue dashed lines determine the upper and lower limits of the 95% confidence interval, respectively. Table 6 gives the equations of the best-fit polynomial lines; their extremely high R^2 (approximately equal to 1) imply an excellent fit to the calculated intra-annual TDI values.

Table 6. Best-fit 6th-order polynomial regression equations for the monthly mean TDIs (in °C); t is the month of the year in the range 1–12; R^2 is the coefficient of determination.

IPCC Scenario, Period	Equation	R^2
RCP 4.5, 2021–2050	$TDI = -0.0003\ t^6 + 0.0127\ t^5 - 0.2110\ t^4 + 1.5271\ t^3 - 4.6786\ t^2 + 6.7114\ t + 6.8759$	0.9997
RCP 4.5, 2046–2075	$TDI = -0.00009\ t^6 + 0.0053\ t^5 - 0.0986\ t^4 + 0.7052\ t^3 - 1.6694\ t^2 + 1.6710\ t + 9.8182$	0.9975
RCP 4.5, 2071–2100	$TDI = -0.0002\ t^6 + 0.0102\ t^5 - 0.1697\ t^4 + 1.1906\ t^3 - 3.2756\ t^2 + 4.0542\ t + 8.7419$	0.9995
RCP 8.5, 2021–2050	$TDI = -0.0003\ t^6 + 0.0138\ t^5 - 0.2226\ t^4 + 1.5943\ t^3 - 4.9267\ t^2 + 7.5063\ t + 5.4503$	0.9991
RCP 8.5, 2046–2075	$TDI = -0.0003\ t^6 + 0.0113\ t^5 - 0.1791\ t^4 + 1.2151\ t^3 - 3.2224\ t^2 + 3.7653\ t + 9.5427$	0.9998
RCP 8.5, 2071–2100	$TDI = -0.0003\ t^6 + 0.0119\ t^5 - 0.2000\ t^4 + 1.4613\ t^3 - 4.5338\ t^2 + 6.7582\ t + 8.6553$	0.9997
historical (1985–2014)	$TDI = -0.0003\ t^6 + 0.0130\ t^5 - 0.2113\ t^4 + 1.4895\ t^3 - 4.3529\ t^2 + 5.9352\ t + 6.6504$	0.9997

Figure 6 repeats the information posed in Figure 3, but in this case the bars refer to the monthly mean TDI differences. In both RCP scenarios the differences are generally reduced during the summer season (JJA) in comparison to the rest of the year. This may be attributed to the fact that the future climate (i.e., the climate change) seems to have a lesser effect on the summer months in comparison to the other seasons. Nevertheless, the increase in TDI under RCP 4.5 is between 0.1 and 1.4 °C and under RCP 8.5 between 0.2 and 2.9 °C. This conclusion excludes the small negative values in January and December (for RCP 8.5 2021–2050) and August (for RCP 4.5 2021–2050); the explanation is not obvious, but it can be taken as a no-real change in the future thermal feeling of the Greek population.

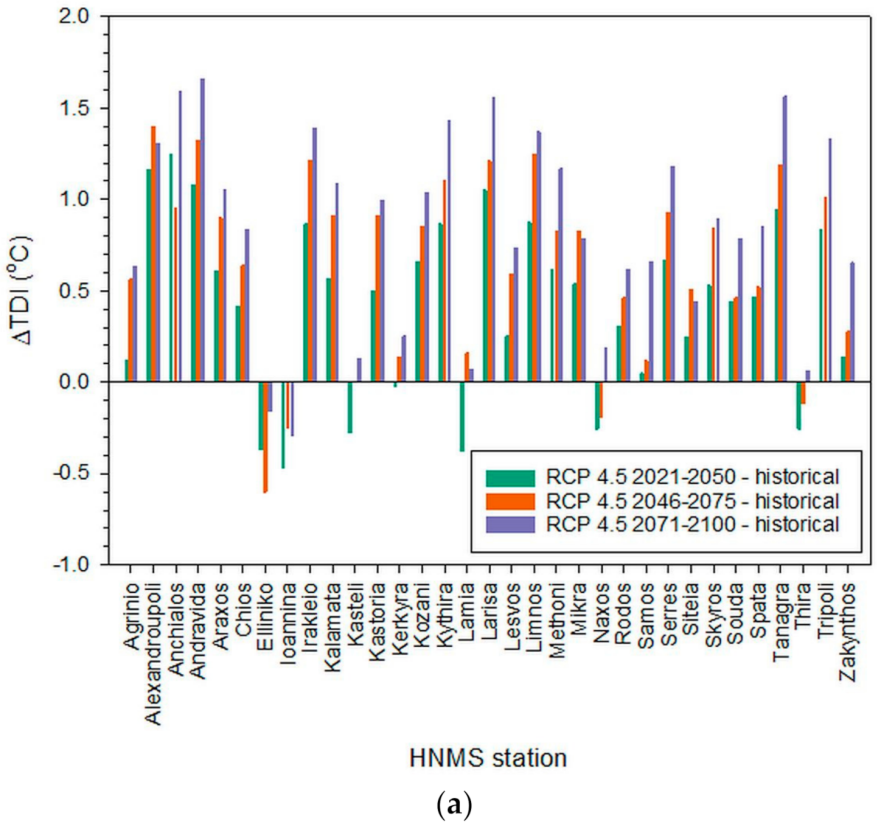

(**a**)

Figure 6. *Cont.*

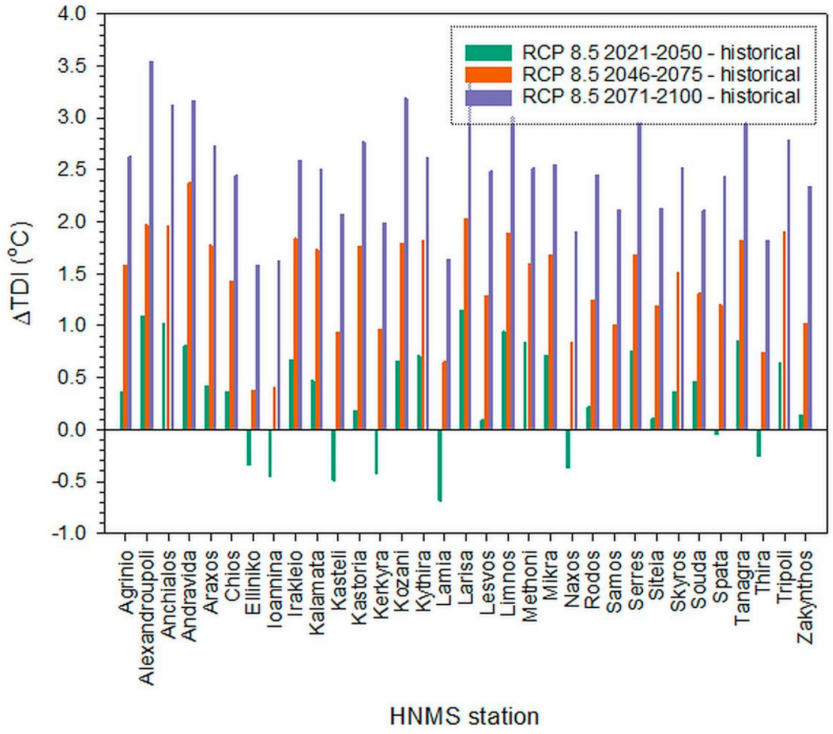

(**b**)

Figure 6. Intra-annual variation of the mean ΔTDIs as derived from the TMYs-MC during the historical period of 1985–2014 and the future epochs of 2021–2050, 2046–2075, 2071–2100 under the (**a**) RCP 4.5 and (**b**) RCP 8.5 IPCC scenarios. The definition of Δ*TDI*s is given in the text.

Some examples of the intra-annual TDI variation for selected sites are given in Figure 7. The selection has been based on the lowest and highest annual TDI values of the site during the various periods encountered in this study. It is seen that Kastoria has always the lowest thermal feeling and its population is not, therefore, in danger in the future in this respect. By contrast, Kythira in most periods and to a lesser extent Rodos and Thira shift their thermal sensation from TDI-class A to TDI-class B in the warm season of the year (June–October).

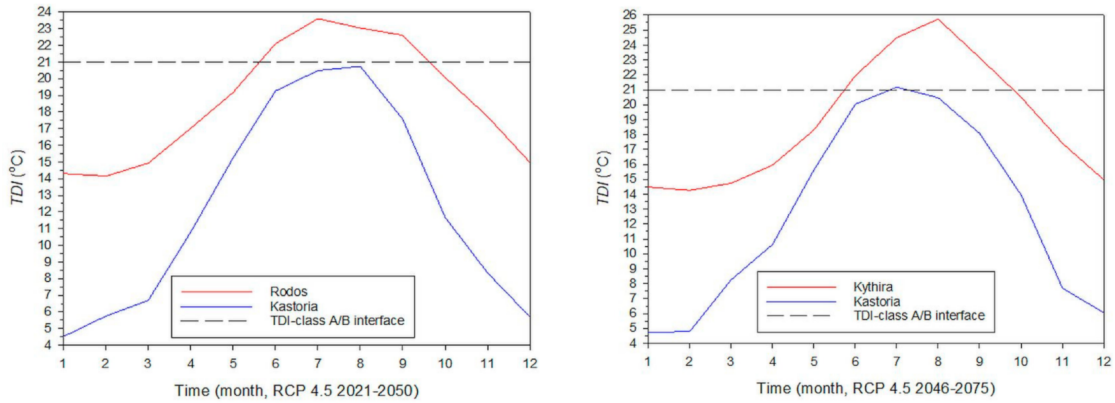

(**a**) (**b**)

Figure 7. *Cont.*

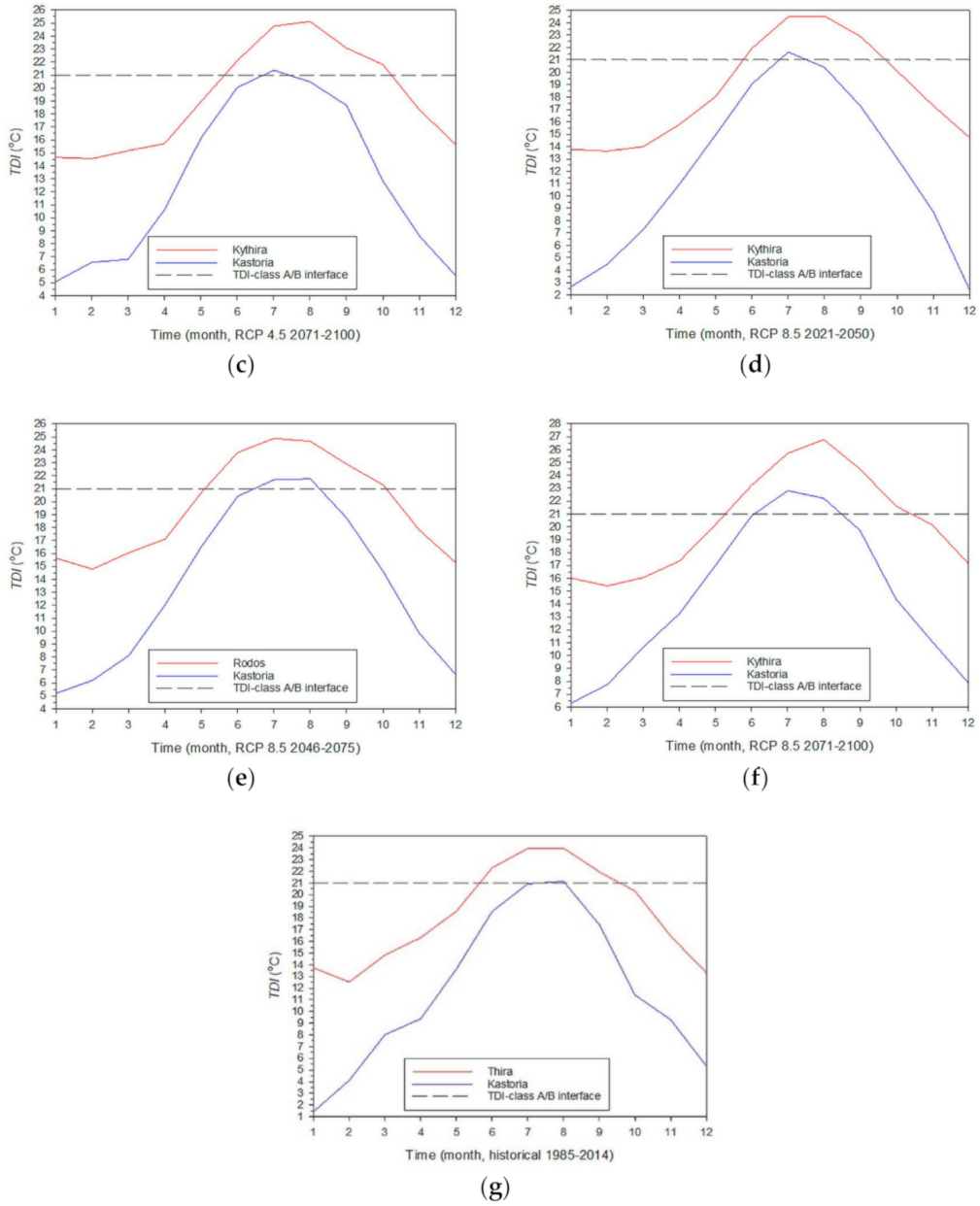

Figure 7. Intra-annual variation of TDI in the epochs: (**a**) RCP 4.5 2021–2050, (**b**) RCP 4.5 2046–2075, (**c**) RCP 4.5 2071–2100, (**d**) RCP 8.5 2021–2050, (**e**) RCP 8.5 2046–2075, (**f**) RCP 8.5 2071–2100, and (**g**) historical 1985–2014 at selected sites in Greece. The dashed lines are the interfaces between the class A (TDI < 21 °C) and class B (TDI ≥ 21 °C).

3.4. Frequency of TDI Occurrence

Up until now, the analysis has not taken into account the various TDI classes; to the contrary all TDI values have been considered from all 33 HNMS sites. This sub-section, however, gives information about the percentage of each TDI-class occurrence in all periods encountered in the study. This is shown in Figure 8. It is remarkable to observe that the TDI-class E (everyone feels thermal discomfort) appears in the historical period and not in any of the future ones, although at a very low percentage. This observation is true as this refers to almost half of the Greek territory (15 sites out of 33, i.e., Agrinio, Alexandroupoli, Anchialos, Kalamata, Kerkyra, Kozani, Lamia, Lesvos, Limnos, Mikra, Serres, Skyros, Souda, Thira, Zakynthos). The interpretation of this finding may be related to higher ambient temperatures in the future, but less humidity (drier weather) over Greece than now. Indeed, Kambezidis et al. [34] have examined the rain data of 31 HNMS stations in the

period 1962–2002 and have found that the rain intensity (in mmh^{-1}) shows (i) higher values in western Greece and lower ones in the Aegean Sea, and (ii) positive trends over Attica, Crete, southern Aegean and negative ones in the rest of the country and especially over the western mainland and Ionian islands. This is also confirmed by [35,36]. Furthermore, a technical report from the Bank of Greece [37] about the future impacts of climate change on various aspects of the Greek economy reports an increase in T_d of 3.4–5.2 °C and a decrease in RH of 1.6–6.8% by 2100.

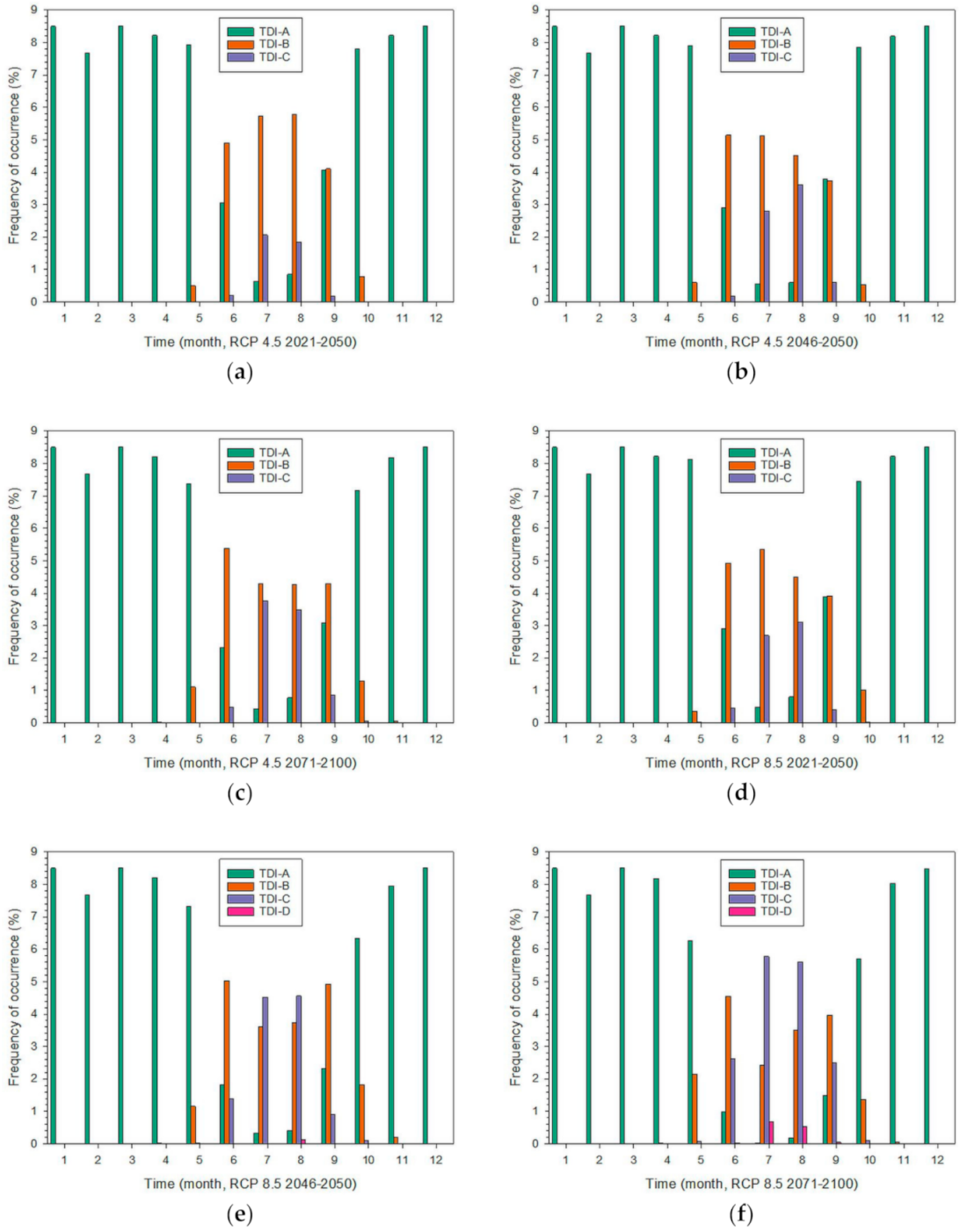

Figure 8. *Cont.*

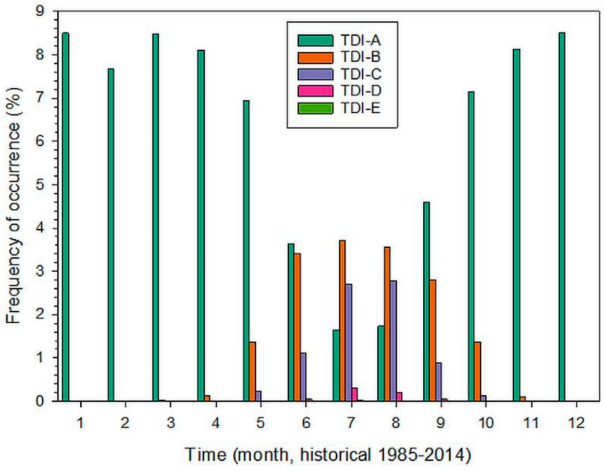

(**g**)

Figure 8. Frequency of occurrence (in %) for the various TDI classes (see Table 1 for definition) across all epochs: (**a**) RCP 4.5 2021–2050, (**b**) RCP 4.5 2046–2075, (**c**) RCP 4.5 2071–2100, (**d**) RCP 8.5 2021–2050, (**e**) RCP 8.5 2046–2075, (**f**) RCP 8.5 2071–2100, and (**g**) historical 1985–2014. The frequencies are averages over all 33 sites in Greece.

3.5. Maps of TDI

Figure 9 contains maps of the annual mean TDI values all over Greece. It is seen that all periods examined present the same pattern, irrespective to the absolute TDI values. Higher TDI values are located in the southern part of Greece, i.e., over south Ionian Sea, the Cyclades, Crete, and Megisti complex east of Rhodes and Crete, while lower TDI values occur in northern Greece and central Peloponnese (see map in Figure 1 for locating these regions). This pattern does not seem to change even in the ultimate future period (2071–2100).

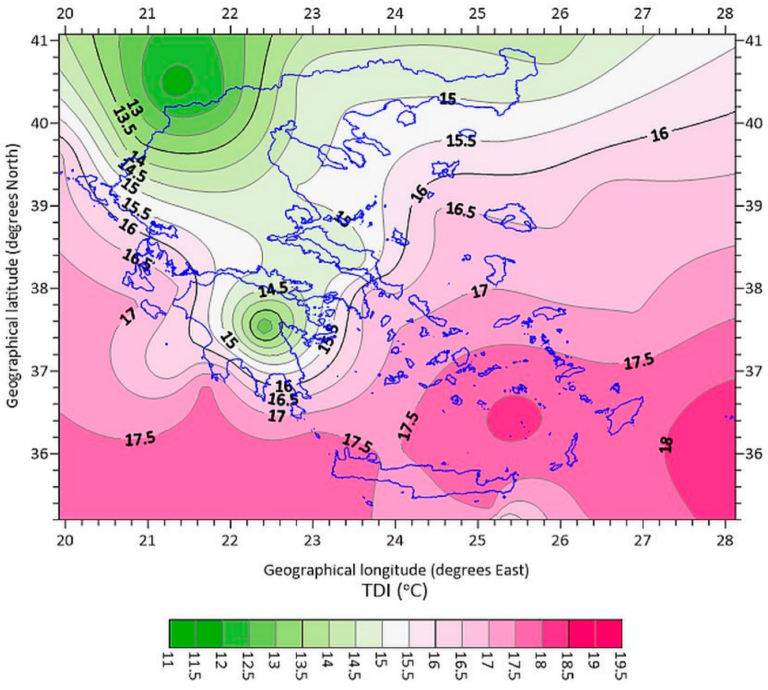

(**a**)

Figure 9. *Cont.*

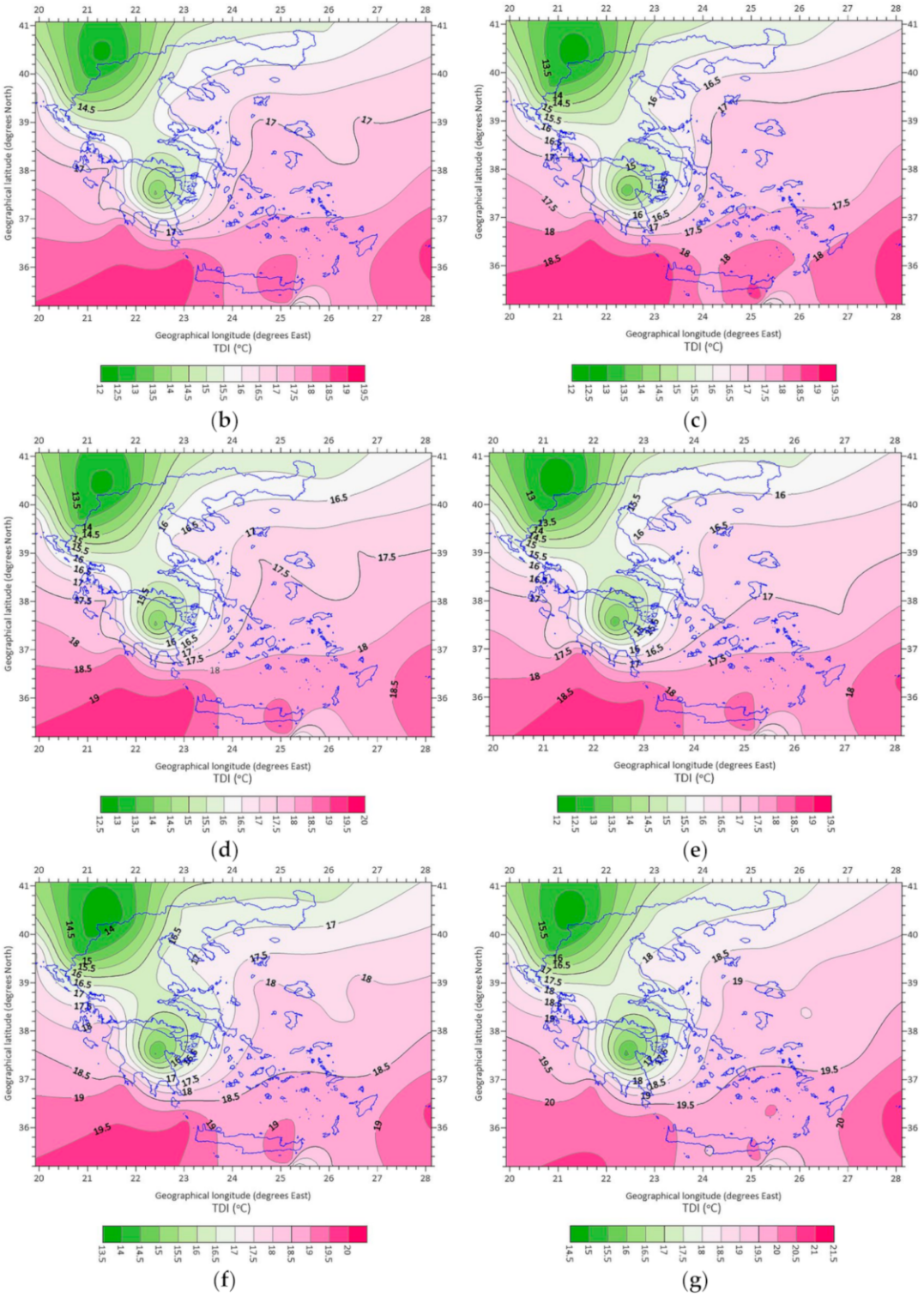

Figure 9. Distribution of annual mean TDI values (in °C) across Greece for the various epochs studied: (**a**) historical 1985–2014, (**b**) RCP 4.5 2021–2050, (**c**) RCP 4.5 2046–2075, (**d**) RCP 4.5 2071–2100, (**e**) RCP 8.5 2021–2050, (**f**) RCP 8.5 2046–2075, and (**g**) RCP 8.5 2071–2100.

4. Discussion

One might wonder whether the relationship between a historical meteorological variable and its evolution in the future is linear or not; in other words, whether there exists such a mathematical relationship for a climatic parameter between now and the

future or, to the contrary, whether the climate-change system is chaotic. As a paradigm, an attempt has been made to answer this question in this study by considering the derivative climatic parameter of TDI. A first look at Equation (1) shows that TDI has a non-linear relationship with the independent variables T_d and RH; so have T_d and RH between each other. Furthermore, if one solves Equation (1) for either T_d or RH, he/she gets a 2nd-order polynomial of T_d or RH as function of the other parameter in the form $y = (ax + b)/(cx + d)$, considering TDI is constant.

$$T_d = (0.7975\ RH + TDI)/(0.0055\ RH + 0.4500), \quad (2)$$

$$RH = (0.4500\ T_d + TDI)/(0.0055\ T_d - 0.7975). \quad (3)$$

From the above expressions, one would, therefore, expect the historical and future TDIs to have a non-linear connection. Nevertheless, Figure 10 shows quite the opposite; there is a fine linear relationship between the historical monthly TDI values and those in any of the other 6 future epochs. No smoothing or deseasonalisation has taken place in the TDI time series. It is worth noticing that the ±95% confidence band around the best-fit line is so narrow that it contains the fewest data points. By contrast, the ±95% prediction zone around the best-fit line includes almost all data points. The difference in interpreting this result is the following. The narrow confidence interval contains some TDI pairs in any of the 6 cases (6 future periods) with a probability of 95%. The existence, however, of the majority of the data pairs outside the confidence interval dictates the fact that the linear best-fit line does not truly represent the relationship of future TDI as function of the historical TDI in the best way. Therefore, one could come to the conclusion that the relationship is not so linear as it appears, but is pseudo-linear. On the other hand, all future TDI pairs will be contained in the prediction interval with a probability of 95%. Then, one could be convinced that the pseudo-linear relation of today will evolve into a linear one in the future. This is confirmed by the high R^2 values in all 6 scatter plots, thus denoting an excellent agreement (correlation) between the historical and future TDI values.

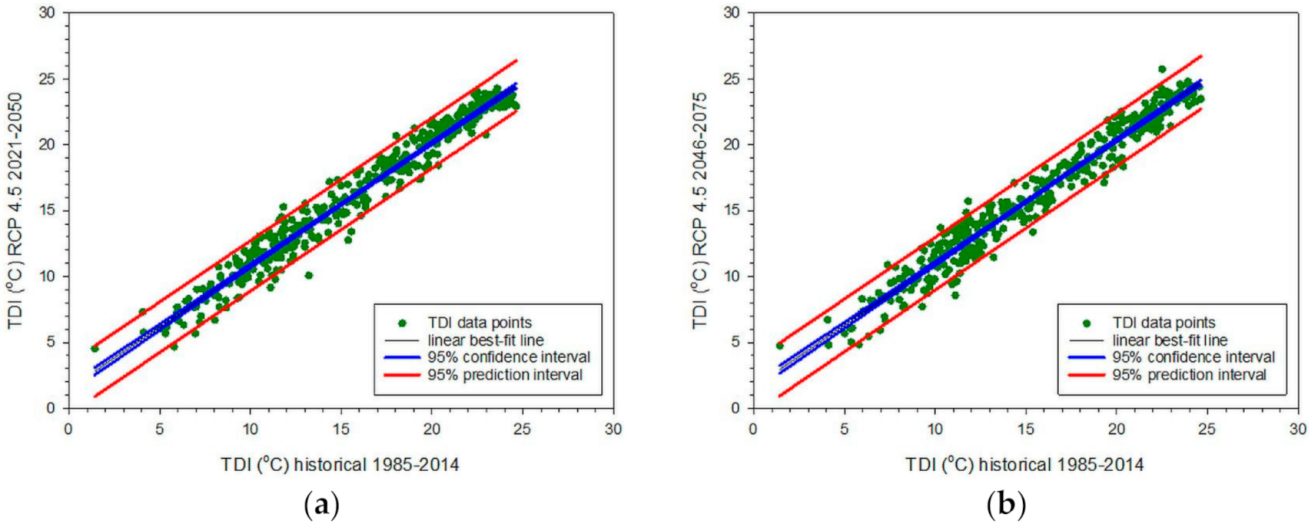

Figure 10. *Cont.*

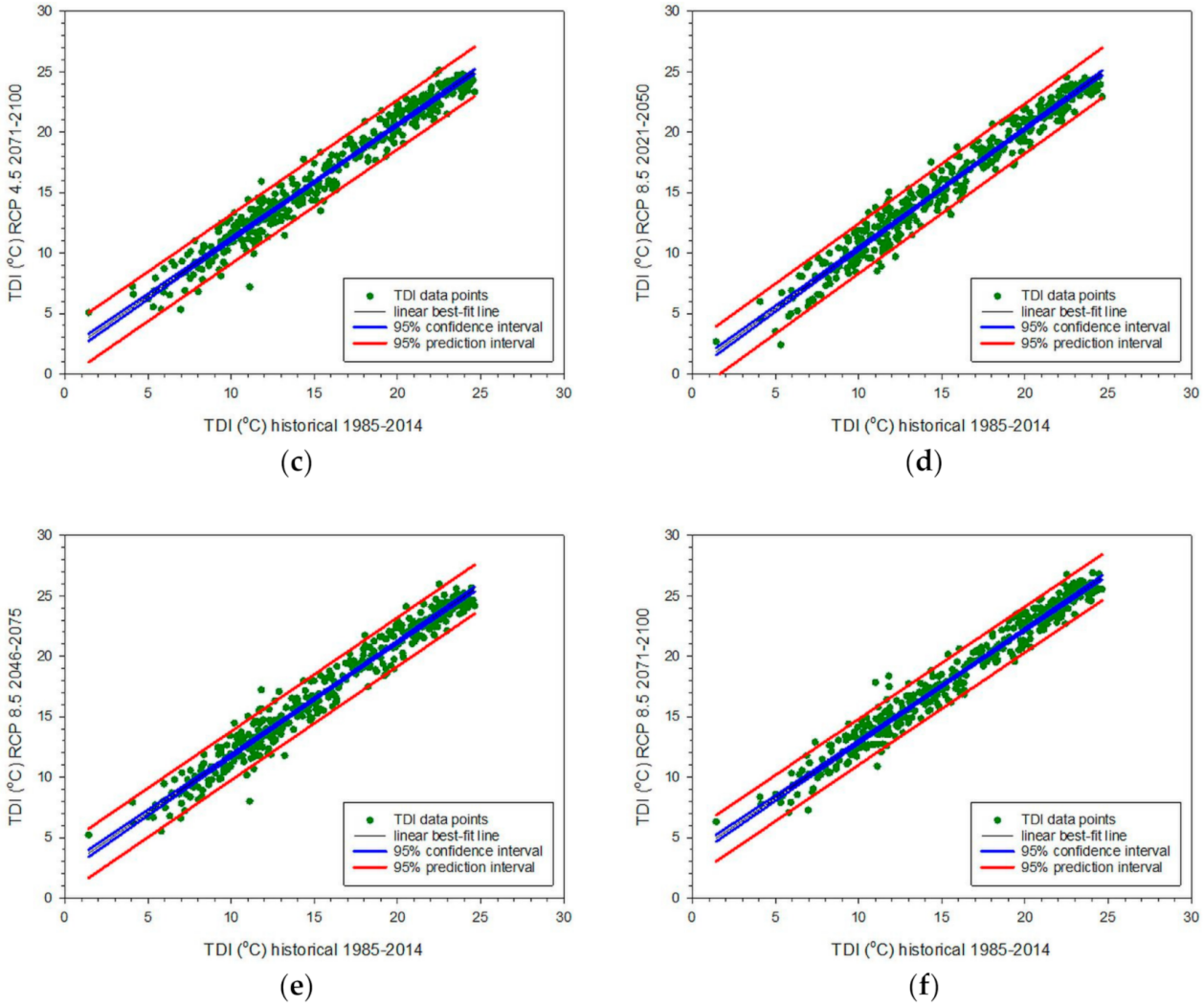

Figure 10. Scatter plots of the monthly mean TDI values averaged over all 33 sites; the x-axis has the TDI values in the historical period and the y-axis in the future epoch of (**a**) RCP 4.5 2021–2050, (**b**) RCP 4.5 2046–2075, (**c**) RCP 4.5 2071–2100, (**d**) RCP 8.5 2021–2050, (**e**) RCP 8.5 2046–2075, and (**f**) RCP 8.5 2071–2100. The solid black line is the best-fit to the data pairs. The 95% confidence and prediction intervals are also shown. R^2 has the following values: (**a**) 0.9635, (**b**) 0.9609, (**c**) 0.9600, (**d**) 0.9626, (**e**) 0.9601, and (**f**) 0.9638.

5. Conclusions

This study investigated the future thermal sensation of the Greek population because of the global-warming effect. Three future periods (2021–2050, 2046–2075, 2071–2100) and two IPCC scenarios (RCP 4.5, RCP 8.5) were chosen for analysis. The thermal (dis)comfort was expressed by Thom's discomfort index (TDI) for 33 sites in Greece. Historical TDI values were also estimated in the period 1985–2014.

The present work presented two innovations. It is the first worldwide (in Greece as well) to (i) compute the future thermal feeling over a country, and (ii) compare it with the past. The second innovation concerns the use of historical as well as future TMYs-MC for all 33 sites, instead of using long-time series of ambient temperature and relative humidity, two parameters that define TDI. The main conclusions of the work can be summarised as follows.

No significant shift from the lowest TDI-class A to the TDI-class B has been shown to occur in the future all over Greece as far as the annual thermal sensation is concerned. TDI was, however, found to increase by ≈0.12 °C/decade, ≈0.11 °C/decade, ≈0.10 °C/decade for the 3 periods under the IPCC RCP 4.5 scenario, and by ≈0.09 °C/decade, ≈0.24 °C/decade,

≈0.30 °C/decade under the IPCC RCP 8.5 one, in comparison with the TDI values in the historical period.

Calculations of the TDI trends during summertime showed an increase of ≈0.03 °C/decade, ≈0.06 °C/decade, ≈0.06 °C/decade for the 3 periods under the IPCC RCP 4.5 scenario, and ≈0.10 °C/decade, ≈0.18 °C/decade, ≈0.25 °C/decade for the respective periods under the IPCC RCP 8.5 scenario, in comparison with the TDI values in the historical period. Such increases were considered insignificant because they did not shift the thermal (dis)comfort from TDI-class B to a higher one, except for the RCP 8.5 2071–2100 period, which was classified in TDI-class C.

For both historical and future epochs best-fit 6th-order regression equations were derived for estimating the monthly mean values of TDI. In all cases R^2 was greater than 0.99.

The decomposition of TDI into its classes and their distribution within the TMYs was performed. It was observed that the TDI-class E (everyone feels thermal discomfort) appeared in the historical period only and not in any future epoch.

Maps of annual mean TDI values were derived; they showed high values over the southern part of Greece (Crete, the Cyclades, south Ionian Sea, Megisti complex), and lower ones over northern Greece and central Peloponnese. This pattern did not seem to change over the decades, from present to future.

A pseudo-linear relationship was shown to exist between the monthly TDI values in any future period with regard to the historical ones. This pseudo-linear expression seemed to evolve into a linear one in the future.

Apart from the conclusions of the present work, it also presents another value: the historical ambient temperature records of 1985–2014 from the 33 sites intrinsically include the recent global surface-warming slowdown, also referred to as hiatus, that occurred in the period 1998–2012 [38].

Author Contributions: Conceptualization, methodology, data curation, data analysis, writing—original draft preparation, writing—review and editing, H.D.K.; future Typical Meteorological Years conceptualization and development through the KRIPIS-THESPIA-II project, software and data curation, B.E.P.; provision of future meteorological and solar radiation data through the KRIPIS-THESPIA-II project, software and data curation K.V.V. and C.G. All authors have read and agreed to the published version of the manuscript.

Funding: This research was implemented in the frame of the KRIPIS-THESPIA-II project, under the grant MIS 5002517, funded by the General Secretariat of Research and Technology in Greece.

Institutional Review Board Statement: Not applicable.

Informed Consent Statement: Not applicable.

Data Availability Statement: The present study was based on meteorological data of 33 sites in Greece provided by the Hellenic National Meteorological Service upon specific request. These data were used to generate the TMYs at the 33 locations.

Acknowledgments: The authors are thankful to the Hellenic National Meteorological Service for providing meteorological data from 33 stations in the network in the period 1985–2014 with the purpose of generating the historical TMYs- MC used in this work through the KRIPIS-THESPIA-II project (WP6). They also express their gratitude to the other members of the KRIPIS-THESPIA-II WP6 team for the generation of the TMYs, both historical and future: Dimitris Kaskaoutis, Kosmas Kavadias, Kalliopi Petrinoli, Ariadne Gavriil, and Dimitris Karagiannis.

Conflicts of Interest: The authors declare no conflict of interest.

Abbreviations

amsl	above mean-sea level
EURO-CORDEX	European Coordinated Regional Climate Downscaling Experiment (Europe)
HNMS	Hellenic National Meteorological Service (Greece)
IERSD	Institute of Environmental Research and Sustainable Development (NOA,Greece)

IPCC	Intergovernmental Panel for Climate Change
MOCI	Mediterranean Outdoor Comfort Index
MPI-M	Max Planck Institute for Meteorology (Germany)
MRM	Meteorological Radiation Model
NOA	National Observatory of Athens (Greece)
NOAA	National Oceanic and Atmospheric Administration (USA)
PET	Popular Events Tracking (model)
PMV	Predicted Mean Vote (model)
RCA	Rossby Centre Regional Atmospheric (model)
RCP	Representative Concentration Pathway
RH	relative humidity
SET	Standard Effective Temperature (model)
SMHI	Swedish Meteorological and Hydrological Institute (Sweden)
TDI	Thom's Discomfort Index
KRIPIS-THESPIA	Development of synergistic and integrated methods and tools for monitoring, management and forecasting of environmental parameters and pressures (research programme, Greece)
TMM	Typical Meteorological Month
TMY	Typical Meteorological Year
WMO	World Meteorological Organisation

References

1. IPCC. *Climate Change 2014: Synthesis Report. Contribution of Working Groups I, II, and III to the 5th Assessment Report of the IPCC*; Pachauti, R.K., Meyer, L.A., Eds.; IPCC: Geneva, Switzerland, 2014.
2. NOAA. Climate at a Glance: Global Time Series 2018. Available online: https://www.ncdc.noaa.gov/cag/ (accessed on 10 December 2020).
3. Sheridan, S.C.; Allen, M.J. Changes in the Frequency and Intensity of Extreme Temperature Events and Human Health Concerns. *Curr. Clim. Change Rep.* **2015**, *1*, 155–162. [CrossRef]
4. Kjellstrom, T.; Briggs, D.; Freyberg, C.; Lemke, B.; Otto, M.; Hyatt, O. Heat, Human Performance, and Occupational Health: A Key Issue for the Assessment of Global Climate Change Impacts. *Annu. Rev. Public Health* **2016**, *37*, 97–112. [CrossRef] [PubMed]
5. Matthews, T. Humid heat and climate change. *Prog. Phys. Geogr. Earth Environ.* **2017**, *42*, 391–405. [CrossRef]
6. Matthews, T.; Wilby, R.L.; Murphy, C. Communicating the deadly consequences of global warming for human heat stress. *Proc. Natl. Acad. Sci. USA* **2017**, *114*, 3861–3866. [CrossRef]
7. Yang, R.; Zhang, H.; You, S.; Zheng, W.; Zheng, X.; Ye, T. Study on the thermal comfort index of solar radiation conditions in winter. *Build. Environ.* **2020**, *167*, 106456. [CrossRef]
8. Adegoke, O.O.; Dombo, T.P. Spatial modelling of human thermal comfort in Akure metropolis using Thom's discomfort index. *Int. J. Environ. Bioenergy* **2019**, *14*, 40–55.
9. Cohen, P.; Potchter, O.; Matzarakis, A. Human thermal perception of Coastal Mediterranean outdoor urban environments. *Appl. Geogr.* **2013**, *37*, 1–10. [CrossRef]
10. Epstein, Y.; Moran, D.S. Thermal comfort and the heat stress index. *Ind. Health* **2006**, *44*, 388–398. [CrossRef]
11. Golasi, I.; Salata, F.; Vollaro, E.D.L.; Coppi, M.; Vollaro, A.D.L. Thermal Perception in the Mediterranean Area: Comparing the Mediterranean Outdoor Comfort Index (MOCI) to Other Outdoor Thermal Comfort Indices. *Energies* **2016**, *9*, 550. [CrossRef]
12. Honjo, T. Thermal comfort in outdoor environment. *Global Environ. Res.* **2009**, *13*, 43–47.
13. Yang, B.; Olofsson, T.; Nair, G.; Kabanishi, A. Outdoor thermal comfort under subarctic climate of north Sweden—A pilot study in Umeå. *Sustain. Cities Soc.* **2017**, *28*, 387–397. [CrossRef]
14. Yousif, T.A.; Tahir, H.M.M. Application of Thom's thermal discomfort index in Khartoum State, Sudan. *J. Forest Prod. Ind.* **2013**, *2*, 36–38.
15. Djongyang, N.; Tchinda, R.; Njomo, D. Thermal comfort: A review paper. *Renew. Sustain. Energy Rev.* **2010**, *14*, 2626–2640. [CrossRef]
16. Angouridakis, V.E.; Makrogiannis, T.J. The Discomfort-Index in Thessaloniki, Greece. *Int. J. Biometeorol.* **1982**, *26*, 53–59. [CrossRef]
17. Giles, B.D.; Balafoutis, C.; Maheras, P. Too hot for comfort: The heatwaves in Greece in 1987 and 1988. *Int. J. Biometeorol.* **1990**, *34*, 98–104. [CrossRef]
18. Paliatsos, A.G.; Nastos, P.T. Relation between air pollution episodes and discomfort index in the greater Athens area, Greece. *Glob. Nest J.* **1999**, *1*, 91–97. [CrossRef]
19. Tselepidaki, I.; Santamouris, M.; Moustris, C.; Poulopoulou, G. Analysis of the summer discomfort index in Athens, Greece, for cooling purposes. *Energy Build.* **1992**, *18*, 51–56. [CrossRef]
20. Tsitoura, M.; Tsoutsos, T.; Daras, T. Evaluation of comfort conditions in urban open spaces. Application in the island of Crete. *Energy Convers. Manag.* **2014**, *86*, 250–258. [CrossRef]

21. Stathopoulou, M.I.; Cartalis, C.; Keramitsoglou, I.; Santamouris, M. Thermal remote sensing of Thom's discomfort index (DI): Comparison with in-situ measurements. *Remote Sens.* **2005**, *5983*, 59830. [CrossRef]
22. Pantavou, K.; Santamouris, M.; Asimakopoulos, D.; Theoharatos, G. Empirical calibration of thermal indices in an urban outdoor Mediterranean environment. *Build. Environ.* **2014**, *80*, 283–292. [CrossRef]
23. Pantavou, K.; Theoharatos, G.; Santamouris, M.; Asimakopoulos, D. Outdoor thermal sensation of pedestrians in a Mediterranean climate and a comparison with UTCI. *Build. Environ.* **2013**, *66*, 82–95. [CrossRef]
24. Katavoutas, G.; Founda, D. Intensification of thermal risk in Mediterranean climates: Evidence from the comparison of rational and simple indices. *Int. J. Biometeorol.* **2019**, *63*, 1251–1264. [CrossRef] [PubMed]
25. Kambezidis, H.D.; Psiloglou, B.E.; Kaskaoutis, D.G.; Karagiannis, D.; Petrinoli, K.; Gavriil, A.; Kavadias, K. Generation of typical meteorological years for 33 locations in Greece: Adaptation to the needs of various applications. *Theor. Appl. Clim.* **2020**, *141*, 1–18. [CrossRef]
26. Thom, E.C. The Discomfort Index. *Weatherwise* **1959**, *12*, 57–61. [CrossRef]
27. Kambezidis, H.D.; Psiloglou, B.E.; Karagiannis, D.; Dumka, U.C.; Kaskaoutis, D.G. Recent improvements of the Meteorological Radiation Model for solar irradiance estimates under all-sky conditions. *Renew. Energy* **2016**, *93*, 142–158. [CrossRef]
28. Kambezidis, H.D.; Psiloglou, B.E.; Karagiannis, D.; Dumka, U.C.; Kaskaoutis, D.G. Meteorological Radiation Model (MRM v6.1): Improvements in diffuse radiation estimates and a new approach for implementation of cloud products. *Renew. Sustain. Energy Rev.* **2017**, *74*, 616–637. [CrossRef]
29. Strandberg, G.; Kjellström, E.; Poska, A.; Wagner, S.; Gaillard, M.-J.; Trondman, A.-K.; Mauri, A.; Davis, B.A.S.; Kaplan, J.O.; Birks, H.J.B.; et al. Regional climate model simulations for Europe at 6 and 0.2 k BP: Sensitivity to changes in anthropogenic deforestation. *Clim. Past* **2014**, *10*, 661–680. [CrossRef]
30. Popke, D.; Stevens, B.; Voigt, A. Climate and climate change in a radiative-convective equilibrium version of ECHAM6. *J. Adv. Model. Earth Syst.* **2013**, *5*, 1–14. [CrossRef]
31. ELOT. *Information and Documentation: Conversion of Greek Characters into Latin Characters*; Standard 743; Hellenic Organisation for Standardisation: Athens, Greece, 2001.
32. ISO. *Information and Documentation: Conversion of Greek Characters into Latin Characters*; Standard 843; International Standardisation Organisation: Geneva, Switzerland, 1997.
33. Papanastasiou, D.K.; Melas, D.; Kambezidis, H.D. Heat waves characteristics and their relation to air quality in Athens. *Global Nest J.* **2014**, *16*, 919–928. [CrossRef]
34. Kambezidis, H.D.; Larissi, I.K.; Nastos, P.T.; Paliatsos, A.G. Spatial variability and trends of the rain intensity over Greece. *Adv. Geosci.* **2010**, *26*, 65–69. [CrossRef]
35. Mimikou, M.A.; Baltas, E.A. Assessment of Climate Change Impacts in Greece: A General Overview. *Am. J. Clim. Change* **2013**, *2*, 46–56. [CrossRef]
36. Giannakopoulos, C.; Kostopoulou, E.; Varotsos, K.V.; Tziotziou, K.; Plitharas, A. An integrated assessment of climate change impacts for Greece in the near future. *Reg. Environ. Change* **2011**, *11*, 829–843. [CrossRef]
37. Commission on the Study of the Climate Change Impacts. *The Environmental, Economic and Social Impacts of Climate Change in Greece*, 1st ed.; Bank of Greece: Athens, Greece, 2011; pp. 68–70. ISBN 978-960-7032-49-2. (In Greek)
38. Tung, K.-K.; Chen, X. Understanding the Recent Global Surface Warming Slowdown: A Review. *Climate* **2018**, *6*, 82. [CrossRef]